

tions through the second excited state is less than 10 percent of those through the first excited state, as expected.

The results on intensity measurements may be summarized by saying that  $35 \pm 5$  percent of the gamma

decays of the capture state proceed by cascade through the first excited state and  $65 \pm 5$  percent by direct transition to the ground state. Less than 4 percent of the gamma decays of the capture state proceed by cascade through the second excited state.

## Angular Distributions of Deuteron-Induced Reactions in Lithium\*

S. H. LEVINE,† R. S. BENDER, AND J. N. MCGRUE  
University of Pittsburgh, Pittsburgh, Pennsylvania

(Received October 25, 1954)

Angular distributions of  $(d,t)$ ,  $(d,He^3)$ ,  $(d,p)$ , and  $(d,d')$  reactions have been obtained using a natural lithium target. Butler type calculations for  $l=1$  transfer fit all of the above data except for the  $(d,d')$  reactions. A  $Q$ -value of  $0.974 \pm 0.015$  Mev has been assigned to the first excited level in Li<sup>8</sup>. The He<sup>6</sup> ground state was observed with the two reactions Li<sup>7</sup> $(d,\alpha)$ He<sup>6</sup> and Li<sup>6</sup> $(d,He^3)$ He<sup>6</sup> for which the  $Q$  values were  $14.26 \pm 0.09$  Mev and  $0.91 \pm 0.09$  Mev, respectively.

### I. INTRODUCTION

A STUDY of the angular distributions of some of the reaction particles resulting from the bombardment of Li<sup>6</sup> and Li<sup>7</sup> with 14.4-Mev deuterons has been made here. The observed angular distributions of the  $(d,t)$ ,  $(d,He^3)$ ,  $(d,p)$ , and  $(d,d')$  reactions are shown. Butler-type calculations<sup>1-3</sup> are used, where possible, to determine the angular momentum transfer and parity change of the reaction. Information about the He<sup>5</sup> ground state is obtained from the two reactions Li<sup>7</sup> $(d,\alpha)$ He<sup>5</sup> and Li<sup>6</sup> $(d,He^3)$ He<sup>5</sup>.

### II. APPARATUS

The scattering project at the University of Pittsburgh<sup>4</sup> uses an incident beam of 14.4-Mev deuterons. The angular spread of the incident beam and of the outgoing particles accepted by the particle analyzer were each  $1.8^\circ$ . A new scattering chamber was installed which could rotate  $60^\circ$  under vacuum. The particle analyzer could be made to cover a continuous range of  $120^\circ$  by changing ports on the scattering chamber. The detector was a CsI crystal cemented to a Type 6292 Dumont photomultiplier tube. The pulse-height resolution was between 4 percent and 6 percent for all charged particles observed. Various aluminum foils could be rotated in front of the crystal to aid in identifying the particles by their pulse height and their energy loss in the foils. Foils also separated pulses of different

particles so that they could be resolved and counted simultaneously with a six-channel pulse-height analyzer.

### III. TARGET PREPARATION

The target was prepared by evaporating natural lithium, which contains 92.5 percent Li<sup>7</sup> and 7.5 percent Li<sup>6</sup>, on a thin silver foil ( $0.01 \text{ mg/cm}^2$ ) in the scattering chamber. Two targets, No. 1 and No. 2, were used during the experiment. The absolute thickness of the targets was measured with a Beckman spectrophotometer, yielding values of  $0.16 \text{ mg/cm}^2$  for target No. 1 and  $0.10 \text{ mg/cm}^2$  for target No. 2. The relative thicknesses as obtained from the magnet spectrometer were in the ratio of 2.1/1.

### IV. RESULTS

#### A. Magnetic Analysis

Table I lists the energy levels observed whose assignments have been uniquely determined by the variation in recoil energy of the outgoing particles with angle except for the  $(d,\alpha)He^5$  and  $(d,He^3)He^5$  reactions. Data for these two reactions were taken at only one angle; however, the  $Q$ -values were such that the detected particles could not have come from any of

TABLE I. List of energy levels and reactions observed. (g.s.  $\equiv$  ground state.)

Reaction	Levels (Mev)
Li <sup>7</sup> $(d,t)$ Li <sup>8</sup>	g.s., 2.187
Li <sup>7</sup> $(d,d')$ Li <sup>7</sup>	g.s., <sup>a</sup> 0.478, 4.61
Li <sup>7</sup> $(d,p)$ Li <sup>8</sup>	g.s., 0.97, 2.28 <sup>a</sup>
Li <sup>7</sup> $(d,He^3)$ He <sup>6</sup>	g.s., 1.71
Li <sup>7</sup> $(d,\alpha)$ He <sup>5</sup>	g.s. <sup>a</sup>
Li <sup>6</sup> $(d,p)$ Li <sup>7</sup>	g.s., 0.478, 6.56 <sup>a</sup>
Li <sup>6</sup> $(d,He^3)$ He <sup>5</sup>	g.s. <sup>a</sup>

<sup>a</sup> Levels observed but angular distribution data not taken.

\* This work was done in the Sarah Mellon Scaife Radiation Laboratory and was assisted by the joint program of the Office of Naval Research and the U. S. Atomic Energy Commission.

† Now at Westinghouse Atomic Power Division Laboratory.

<sup>1</sup> H. C. News, Proc. Phys. Soc. (London) **A65**, 916 (1952).

<sup>2</sup> S. T. Butler, Proc. Roy. Soc. (London) **A208**, 559 (1951).

<sup>3</sup> R. Huby and H. C. News, Phil. Mag. **42**, 1442 (1952).

<sup>4</sup> Bender, Reilley, Allen, Ely, Arthur, and Hausman, Rev. Sci. Instr. **23**, 542 (1952).

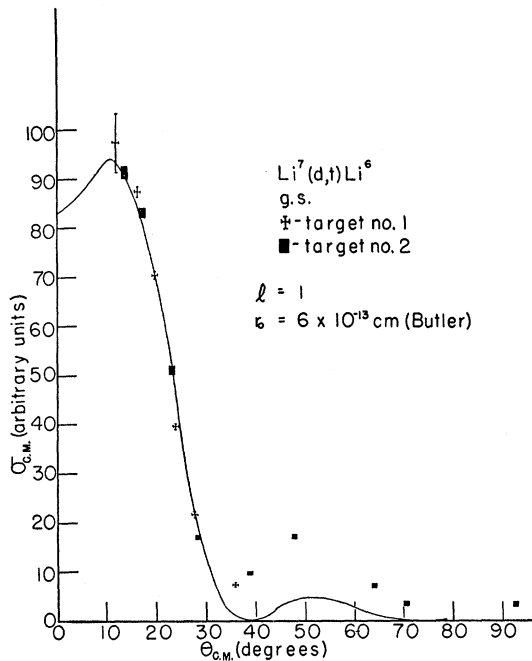


Fig. 1. Angular distribution of the  $\text{Li}^7(d,t)\text{Li}^6$  ground-state reaction.

the contaminants. All levels listed have been reported previously.<sup>5</sup>

Data taken at the laboratory angle of  $8.6^\circ$  had to be corrected, since at this angle the Faraday cage was

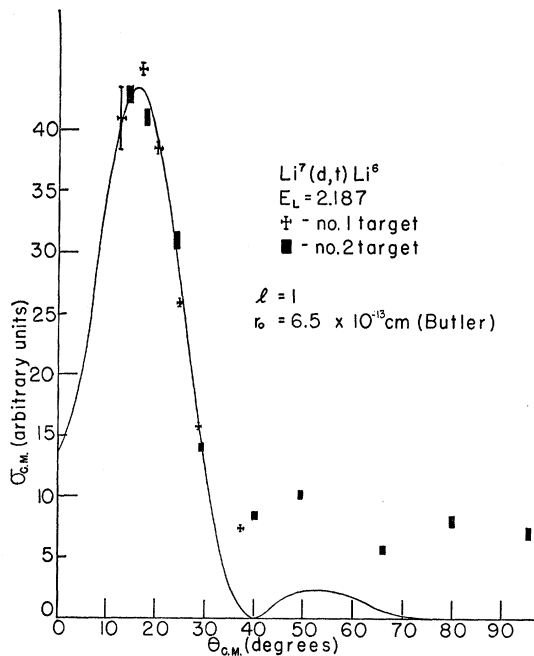


Fig. 2. Angular distribution of the  $\text{Li}^7(d,t)\text{Li}^6$  2.187 level.

<sup>5</sup> F. Ajzenberg and T. Lauritsen, *Revs. Modern Phys.* **24**, 321 (1952).

partially blocking the used sector of No. 3 magnet. A correction of 12 percent was made from the geometry of the system; the uncertainty of this correction introduced an error of  $\pm 6$  percent. This accounts for the large error at the most forward points of each angular distribution.

The solid angle  $\Omega$  of the particle analyzer was measured experimentally by observing the ratio of Po  $\alpha$  particles counted by a known solid angle to that counted by the analyzer. The measured solid angle  $\Omega = 1.77 \times 10^{-4}$  steradian agreed with the geometric solid angle of  $1.8 \times 10^{-4}$  steradian. The absolute cross section of the elastically scattered deuterons was compared with the Rutherford scattering cross section at an angle of  $36^\circ$  in the center-of-mass system. The

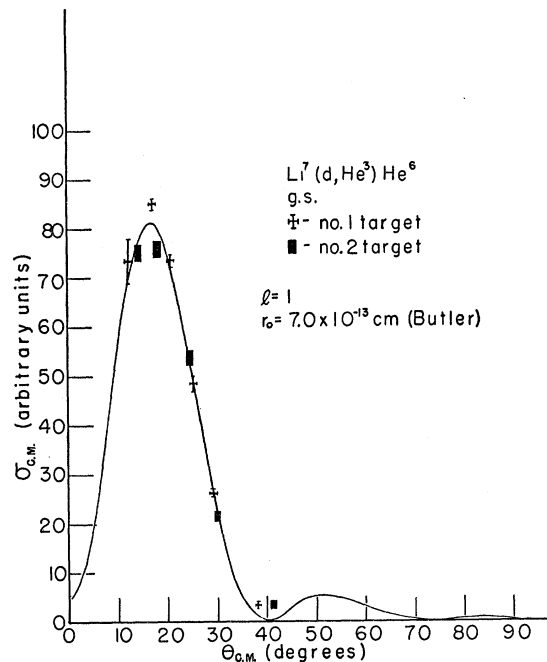


Fig. 3. Angular distribution of the  $\text{Li}^7(d,\text{He}^3)\text{He}^6$  ground-state level.

Rutherford scattering cross section was found to be smaller by a factor of four.

Using the silver backing material as a target, a survey run at an angle of  $16^\circ$  showed that the silver made no contribution to the lithium cross sections.

### B. $\text{Li}^7(d,t)\text{Li}^6$

The two triton groups observed correspond to the  $\text{Li}^6$  ground state and the 2.187-Mev level. At the most forward angles the magnetic field required to focus the tritons was so great as to be out of range of the proton resonance equipment. For these cases, the proton resonance frequency was obtained in the following manner. Since the current in the magnet coils could also be measured using a potentiometer dial reading, a

graph of potentiometer dial reading *versus* proton resonance frequency was drawn. This graph was then extended beyond the range of the proton resonance frequency, 61 Mc/sec, to 66 Mc/sec from which all the necessary data could be obtained. Tritons from the  $\text{Li}^6$  3.58-Mev level were not observed. This might be attributed to the fact that at the most forward angles where the cross sections are relatively greater, the elastic peak appeared at the same value of the magnetic field as would tritons from the  $\text{Li}^6$  3.58-Mev level; the intensity of the elastic peak made such observations impossible.

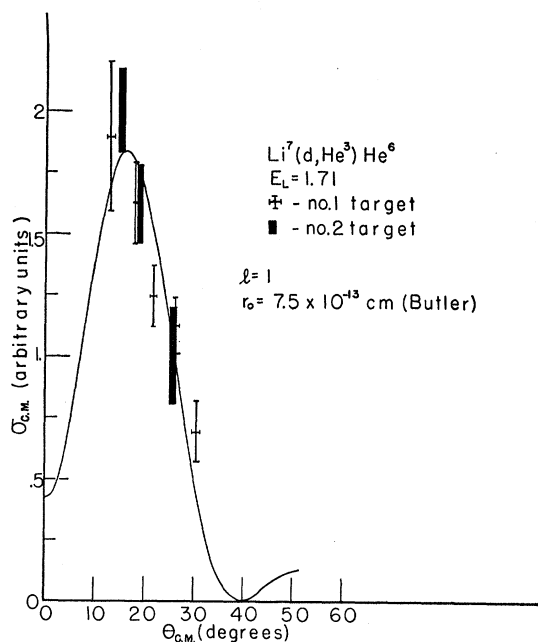


FIG. 4. Angular distribution of the  $\text{Li}^7(d, \text{He}^3)\text{He}^6$  1.71 level.

### 1. $\text{Li}^6$ Ground State

The angular distribution in the center-of-mass system for the triton group corresponding to the ground state of  $\text{Li}^6$  is shown in Fig. 1. The solid line is the Butler curve for  $l=1$  and radius  $r_0 = 6 \times 10^{-13}$  cm. Holt and Marsham<sup>6</sup> have previously reported the angular distribution of this reaction using an incident deuteron energy of approximately 7.7 Mev. Normalizing their peak to the peak of the data presented here produces a similar distribution displaced toward the larger angles. A larger radius, however, is needed to fit their data.

### 2. $\text{Li}^6$ 2.187-Mev Level

The solid line in Fig. 2 is the Butler curve for  $l=1$  and  $r_0 = 6.5 \times 10^{-13}$  cm.

<sup>6</sup> J. R. Holt and T. N. Marsham, Proc. Phys. Soc. (London) **66A**, 1032 (1953).

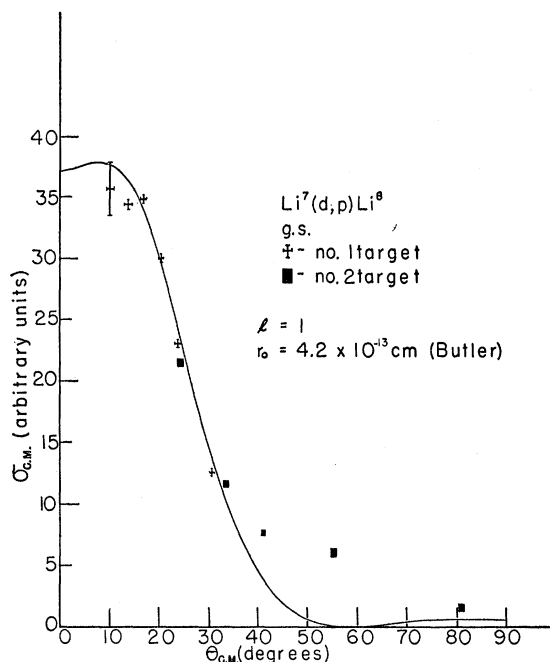


FIG. 5. Angular distribution of the  $\text{Li}^7(d, p)\text{Li}^8$  ground state.

## C. $\text{Li}^7(d, \text{He}^3)\text{He}^6$

### 1. $\text{He}^6$ Ground State

The angular distribution of this reaction is shown in Fig. 3. The best fit is obtained with a radius of  $7 \times 10^{-13}$  cm and  $l=1$ .

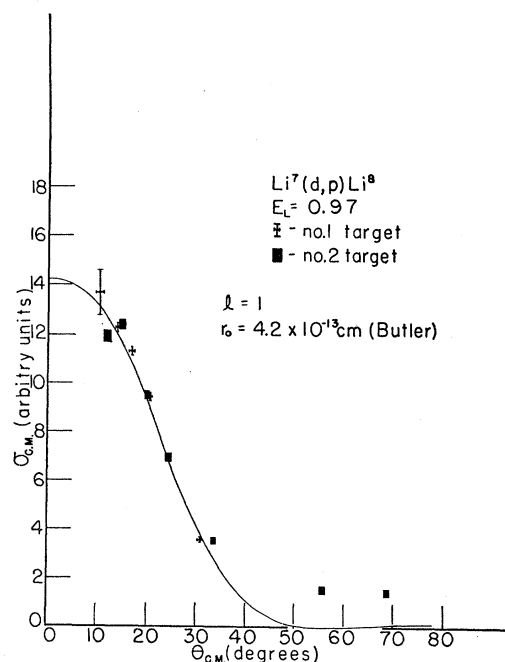
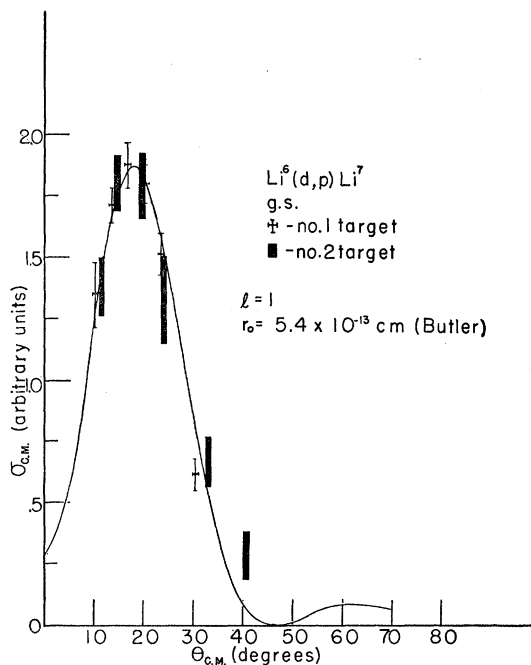
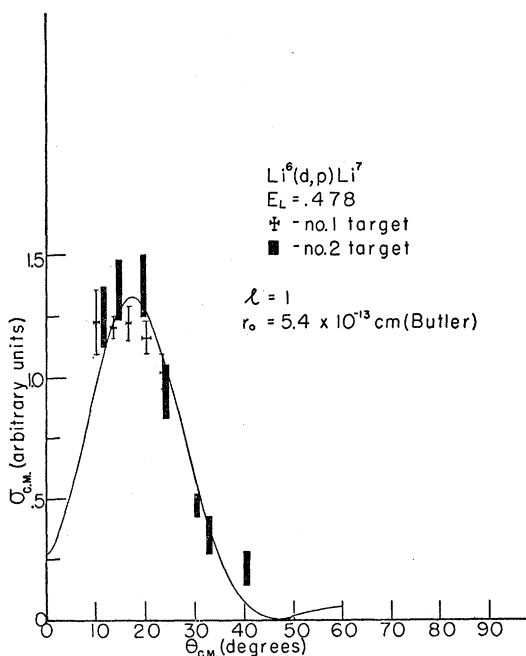


FIG. 6. Angular distribution of the  $\text{Li}^7(d, p)\text{Li}^8$  0.97 level.

FIG. 7. Angular distribution of the  $\text{Li}^6(d,p)\text{Li}^7$  ground state.

### 2. $\text{He}^6$ 1.71-Mev Level

The angular distribution of this reaction is shown in Fig. 4. A Butler curve of  $l=1$  and  $r_0=7.5 \times 10^{-13}$  cm gives a fit to the data.

FIG. 8. Angular distribution of the  $\text{Li}^6(d,p)\text{Li}^7$  0.478 level.

## D. $\text{Li}^7(d,p)\text{Li}^8$

### 1. $\text{Li}^8$ Ground State

For this reaction a correction for the contaminant peak,  $\text{C}^{13}$  3.08-Mev level, underneath the  $\text{Li}^8$  ground state had to be made at the most forward angles. The two targets had different amounts of carbon deposits giving two different angular distributions for the  $\text{Li}^8$  ground-state reaction. The difference between the two curves yielded the angular distribution of the contaminant peak. A correction could therefore be made for the contaminant peak contribution. The Butler curve for  $l=1$  and  $r_0=4.2 \times 10^{-13}$  cm gave the best fit to the experimental data as shown in Fig. 5.

The angular distribution of this reaction has been previously reported by Holt and Marsham<sup>6</sup> who used 7.7-Mev incident deuterons. They ascribed an  $l=1$  transfer to this reaction; however, they were unable to fit the data exactly with a Butler curve. The shape of their distribution was such that two different radii,  $r_0=5.3 \times 10^{-13}$  cm and  $r_0=4.0 \times 10^{-13}$  cm, gave equally good results.

TABLE II. Energy values observed for the  $\text{Li}^8$  0.97-Mev level at various angles.

$\theta_{\text{lab}}$ (degrees)	Level values (Mev)
15	0.973
22.3	0.974
11	0.965
12.1	0.974
11.6	0.970
8.6	0.971
14.1	0.974
17.1	0.977
17.1	0.975
19.9	0.980
25.9	0.976
12.4	0.976

### 2. $\text{Li}^8$ 0.97-Mev Level

Data for this reaction were taken at 11 different angles; the possibility that this level could have been a contaminant level was ruled out by the angular dependence of the level spacing from the  $\text{Li}^8$  ground state which is a sensitive function of the assumed target nucleus. Data for this level are presented in Table II. The average of the values in Table II assign to this level a value of  $0.974 \pm 0.015$  Mev.

The Butler curve for  $l=1$  and  $r_0=4.2 \times 10^{-13}$  cm gave the best fit to the data taken for this reaction as shown in Fig. 6.

## E. $\text{Li}^6(d,p)\text{Li}^7$

Holt and Marsham<sup>6</sup> have obtained angular distributions of the  $\text{Li}^6(d,p)\text{Li}^7$  ground state and 0.478-Mev levels as far forward as  $0^\circ$ . They used values of  $l=1$  and  $r_0=4.9 \times 10^{-13}$  cm for the Butler curve.

1.  $Li^7$  Ground State

Figure 7 shows that a Butler curve for  $l=1$  and  $r_0=5.4 \times 10^{-13}$  cm fits the data.

2.  $Li^7$  0.478-Mev Level

Figure 8 shows the fit obtained with a Butler curve using values  $l=1$  and  $r_0=5.4 \times 10^{-13}$  cm.

F.  $Li^7(d,d')Li^7$

1.  $Li^7$  0.478-Mev Level

Figure 9 shows the Huby and Newns<sup>3</sup> theory for  $l=2$  and  $r_0=6.5 \times 10^{-13}$  cm and the experimental data.

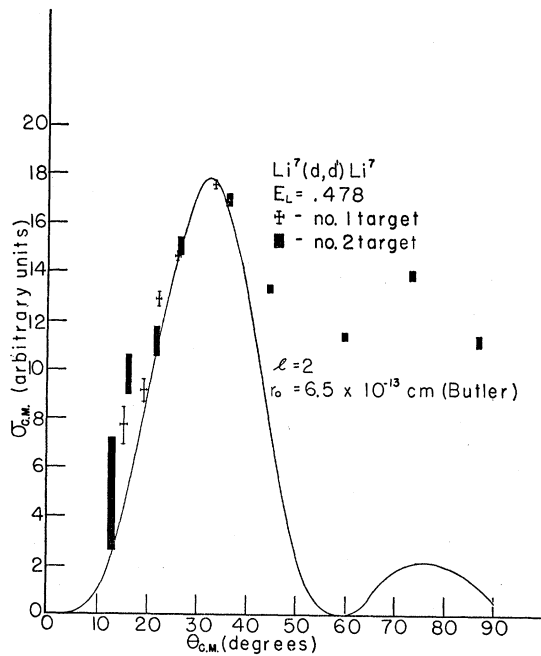


FIG. 9. Angular distribution of the  $Li^7(d,d')Li^7$  0.478 level.

This value of  $l$  is consistent with the results obtained from the  $Li^6(d,p)Li^7$  0.478-Mev reaction. Slit edge scattering increased rapidly toward smaller angles and at the same time the cross section decreased producing large errors for this reaction at the forward angles.

2.  $Li^7$  4.61-Mev Level

Figure 10 shows only the experimental points since no values of the parameters in the Huby and Newns theory produced a reasonable fit to the data.

A search for the  $Li^6(d,p)Li^7$  4.61-Mev level was made only at angles less than  $20^\circ$  in the laboratory system, because at angles greater than  $20^\circ$ , proton groups from other elements appeared at the same magnetic field setting. This reaction was not observed although a differential cross section greater than 3 mb would have permitted its observation.

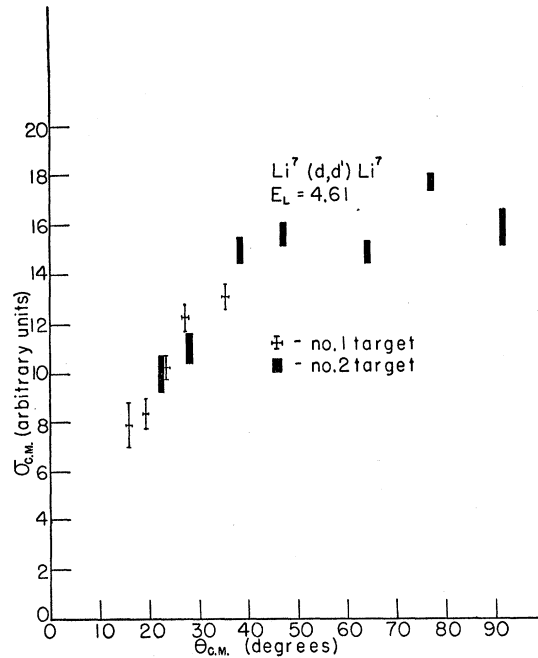


FIG. 10. Angular distribution of the  $Li^7(d,d')Li^7$  4.61 level.

Three values of the  $Q$  of the  $Li^7(d,d')Li^7$  4.61-Mev reaction were  $-4.60$ ,  $-4.62$ , and  $-4.63$  Mev yielding an average  $Q$ -value  $= -4.62 \pm 0.04$  Mev. The width of the peak,  $\Delta E$ , at half-maximum in the laboratory

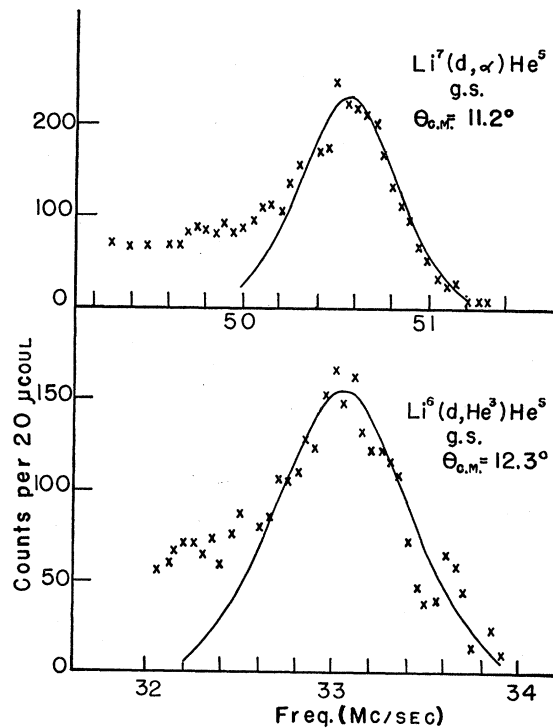


FIG. 11. Counts per 20 microcoulombs as a function of analyzing magnet field for the  $Li^7(d,\alpha)He^5$  ground state and the  $Li^6(d,He^3)He^5$  ground state.

TABLE III. Summary of results obtained. (g.s.≡ground state.)

Reaction	$l$	Spin (parity)	$r_0 \times 10^{-13}$ cm	$Q$ (Mev)	$\sigma(\theta)$ mb/sterad	$\theta$ (c.m.)	$\Delta Q$ (Mev)
$\text{Li}^7(d,t)\text{Li}^6$ g.s.	1	$1^+$	6.0		32.4	$11^\circ$	
$\text{Li}^7(d,t)\text{Li}^6$ 2.187 Mev	1	$3^+$	6.5		16.0	$16^\circ$	
$\text{Li}^7(d,p)\text{Li}^8$ g.s.	1	$0^+, 1^+, 2^+, 3^+$	4.2		26.1	$8^\circ$	
$\text{Li}^7(d,p)\text{Li}^8$ 0.97 Mev	1	$0^+, 1^+, 2^+, 3^+$	4.2	- 1.162	10.2	$2^\circ$	
$\text{Li}^7(d,\text{He}^3)\text{He}^6$ g.s.	1	$0^+$	7.0		8.0	$17^\circ$	
$\text{Li}^7(d,\text{He}^3)\text{He}^6$ 1.71 Mev	1	$0^+, 1^+, 2^+, 3^+$	7.5		2.0	$16.5^\circ$	
$\text{Li}^7(d,\alpha)\text{He}^5$ g.s. <sup>a</sup>				14.26	2.1	$11.2^\circ$	0.66
$\text{Li}^6(d,\text{He}^3)\text{He}^5$ g.s. <sup>a</sup>				0.91	32.0	$12.3^\circ$	0.69
$\text{Li}^6(d,p)\text{Li}^7$ g.s.	1	$\frac{3}{2}^-$	5.4		12.8	$18^\circ$	
$\text{Li}^6(d,p)\text{Li}^7$ 0.478 Mev	1	$\frac{1}{2}^-$	5.4		9.2	$17.5^\circ$	
$\text{Li}^6(d,p)\text{Li}^7$ 6.56 Mev <sup>a</sup>				0.91	32.0	$12.3^\circ$	0.67
$\text{Li}^7(d,d')\text{Li}^7$ g.s. <sup>a</sup>					7.7	$32^\circ$	
$\text{Li}^7(d,d')\text{Li}^7$ 0.478 Mev					8.8	$47^\circ$	
$\text{Li}^7(d,d')\text{Li}^7$ 4.61 Mev				- 4.62			0.3

<sup>a</sup> Levels observed but angular distribution data not taken.

system was found to be  $0.3 \pm 0.1$  Mev corresponding to a  $\Delta Q$  of  $0.3 \pm 0.1$  Mev.

### G. Ground State of $\text{He}^5$

The  $\text{Li}^7(d,\alpha)\text{He}^5$  and the  $\text{Li}^6(d,\text{He}^3)\text{He}^5$  reactions were observed to lead to the  $\text{He}^5$  ground state. Figure 11 shows the observed counting rate as a function of proton resonance frequency, the high-energy part of the data having been fitted with a Gaussian curve. The  $(d,\text{He}^3)$  reaction data have been plotted with a gamma-ray background of 31 counts subtracted from each point. Both levels are very broad having asymmetrical shapes that indicate three-body disintegration.<sup>7</sup> By correcting the observed level widths for the instrumental contributions, the resulting widths of the fitted Gaussian at half-maximum of the  $\text{Li}^7(d,\alpha)\text{He}^5$  and the  $\text{Li}^6(d,\text{He}^3)\text{He}^5$  reactions in the laboratory system were 0.48 Mev and 0.62 Mev respectively. The corresponding  $\Delta Q$ 's are  $0.66 \pm 0.20$  Mev and  $0.69 \pm 0.20$  Mev. The  $Q$ -values obtained for these reactions were  $14.26 \pm 0.09$  Mev for the  $(d,\alpha)$  reaction and  $0.91 \pm 0.09$  Mev for the  $(d,\text{He}^3)$  reaction, corresponding to mass defects of 12.82 Mev and 12.86 Mev.

The absolute differential cross sections obtained at center-of-mass angles of  $11.2^\circ$  for the  $(d,\alpha)$  reaction and  $12.3^\circ$  for the  $(d,\text{He}^3)$  reaction were

$$\sigma(\theta)_\alpha = 2.1 \pm 0.7 \text{ mb/sterad,}$$

and

$$\sigma(\theta)_{\text{He}^3} = 32 \pm 13 \text{ mb/sterad.}$$

### V. DISCUSSION

The errors in the relative cross section were computed for each point. Statistical variation in counts and errors

in background subtraction accounted for most of the errors. An additional error of 2 percent was introduced for those triton peaks which were focused by magnetic fields too large to be measured with the proton resonance equipment. The error in the absolute cross section was due almost entirely to an estimated uncertainty of 25 percent in the target thickness.

Either Born or Butler type calculations provide satisfactory fits to the observed angular distributions resulting from pickup reactions at angles smaller than  $35^\circ$  (c.m.). In the pickup calculations a Gaussian wave function was used for the internal wave function of the triton or  $\text{He}^3$  particle. A single radius was employed to fit the Butler curves to the angular distributions of the  $(d,p)$  reactions involving the same final nucleus. The radius  $r_0 = 4.2 \times 10^{-13}$  cm used with the  $\text{Li}^8$  angular distributions comes close to the value  $4.1 \times 10^{-13}$  cm obtained using the Gamow and Critchfield formula. Butler type calculations for  $l=1$  transfer provide the best fit to all the above data. Neither  $l=0$  or  $l=2$  transfer provided a satisfactory fit. In all cases the  $l$  values are consistent with the known data.

Table III summarizes the majority of the results obtained from this experiment. The article of Ajzenberg and Lauritsen<sup>5</sup> was used in preparing the column listing spin and parity. It lists the reactions observed, the  $l$  transfer for each reaction, the parity and possible spin values of the final state, the radius  $r_0$ , the measured  $Q$ -values for the particular reaction, the absolute differential cross section  $\sigma(\theta)$  with the corresponding angle in the center-of-mass system, and the width at half-maximum  $\Delta Q$ .

We wish to acknowledge the help received from Dr. A. J. Allen, Dr. E. Gerjuoy, Mr. W. F. Vogelsang, and Mr. E. K. Warburton, as well as from the many other members of the Laboratory who have taken interest in this project.

<sup>7</sup> C. D. Moak, Phys. Rev. **92**, 383 (1953).